

Piecewise adiabatic population transfer in a molecule via a wave packet

Evgeny A. Shapiro¹, Avi Pe'er⁴, Jun Ye⁴, Moshe Shapiro^{1,2,3}

Departments of ¹Chemistry and ²Physics, The University of British Columbia, Vancouver, V6T 1Z2, Canada,

³Department of Chemical Physics, The Weizmann Institute, Rehovot, 76100, Israel,

⁴JILA, National Institute of Standards and Technology and University of Colorado, Boulder, CO 80309-0440, USA.

(Dated: January 26, 2023)

We propose a new class of control schemes for robust transfer of population between quantum states via a wave packet that utilize trains of coherent pulses (optical frequency comb). Our approach draws from analogy to adiabatic passage techniques, but is more general. Transfer can be implemented by a piecewise Stimulated Raman Adiabatic Passage, which uses pulse trains with pulse-to-pulse amplitude variation, or by a piecewise chirped Raman passage with pulse-to-pulse phase variation. Viewed in the spectral domain, these techniques rely on quantum pathway interference in an adiabatic passage. In the context of production of ultracold ground-state molecules, we show that with no *a-priori* knowledge of the excited potential structure, robust high-efficiency Raman transfer is possible, by scanning the repetition rate and carrier phase of the excitation comb.

PACS numbers: 42.50.Hz, 82.50.Nd, 82.53.Kp, 34.50.Cx

With the advent of novel quantum technologies, there is a need for methods of controlling quantum systems that are, on one hand, robust and conceptually simple, and on the other, flexible and applicable far beyond the few-level arrangements found in textbooks. This work is aimed towards development of one family of such methods. Our goal is to utilize the intuition and control recipes of simple schemes for robust transfer of quantum population based on Adiabatic Passage (AP), and apply them to the situations involving many-level quantum systems with complex wave packet dynamics. The key components of the method are coherent accumulation by a train of phase coherent optical pulses, and interference of quantum pathways in multi-state population transfer.

While the concept of coherent accumulation has been well studied in the context of spectroscopy and perturbative control [1], two previous publications studied its use for complete population transfers. One was the analysis within the 3 level model of piecewise adiabatic passage (PAP) - an adiabatic passage performed with a coherent train of pulses [2]. The other demonstrated population transfer through a wave packet with a coherent train of pump-dump pulses [3]. In this Letter, we unite the two as special cases within one general framework, where the combination of adiabatic transfer concepts with a coherent train excitation (optical frequency comb) leads to a class of schemes that preserves the robustness of adiabatic transfer, but is applicable for population transfers that involve composite quantum states.

The concept of piecewise adiabaticity is elucidated with two main examples. In piecewise stimulated Raman adiabatic passage (STIRAP), robust transfer is achieved through a slow variation of the intensity envelope of the driving pulse trains. In the other, which we term “chirped Raman passage” (CRP), robustness is obtained by slow variation of the excitation phase. We then demonstrate how both examples can be extended to the case of the intermediate state being a wave packet, i.e. a

multiplicity of intermediate states. Specifically we show how the excitation can be tailored to the intermediate dynamics to achieve near unity transfer efficiencies. In the spectral domain, the transfer is seen as a constructive interference of several AP pathways [4, 5]. Last, we discuss the case of transfer without detailed knowledge of the intermediate dynamics. We show that by scanning the comb parameters of a train of unshaped pulse-pairs (repetition rate and intra-pair time separation) it is still possible to achieve high efficiency transfer. The intermediate dynamics can then be studied using a two-dimensional mapping of the transfer efficiency as a function of the comb parameters.

A traditional AP allows to transfer population from an initial to a target state of a quantum system by dressing the system in slowly changing fields, and making one of the time-dependent field-dressed eigenstates coincide with the initial state at the beginning of the process, and with the target at the end [5, 6, 7]. The AP transfer is complete and robust as long as the dressing fields change adiabatically. Accordingly, the prescription of a Piecewise Adiabatic Passage (PAP) [2] can be summarized as follows: As reference, consider any traditional AP, driven by slowly varying dressing fields. Then, break the reference AP into a set of time intervals τ_n , so short that only a small fraction of population is transferred between the eigenstates during each interval. Within each interval, the driving fields can be replaced by *any other* field amplitude shape, as long as the integral action of each of the fields over τ_n remains the same. For example, the smooth reference field can be replaced by a train of mutually coherent pulses. Last, vary the inter-pulse ‘silent’ time of system’s free evolution. Controlling the durations of the periods of free evolution and the phase of each of the driving fields allows control over the arising Ramsey-type interference picture.

Ref. [2] introduced piecewise versions of STIRAP [6, 7], which transfers population in a three-level system from

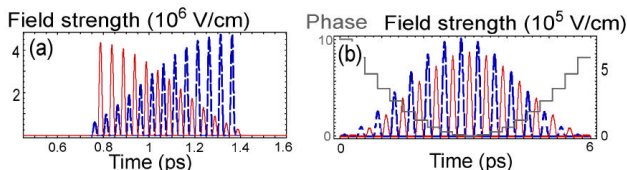


FIG. 1: (Color online). Sequences of femtosecond pulses able to drive piecewise STIRAP (a) and piecewise CRP (b) between the states $|1\rangle = 3s$, $|2\rangle = 4p$, and $|3\rangle = 5s$ of atomic Na [8]. Dashed blue: pump field envelope; solid red: dump envelope; gray: the phase of the carrier in piecewise CRP with $\alpha_P = \alpha_D = 0.2$.

state $|1\rangle$ into state $|3\rangle$ via the intermediate $|2\rangle$. In the key example, the field was given as a train of femtosecond “pump” and “dump” pulse pairs, resonantly coupling, respectively, the eigenstates $|1\rangle$ and $|2\rangle$ (pump), and the eigenstates $|2\rangle$ and $|3\rangle$ (dump). The pulses – “kicks” – did not overlap in time and the pulse train envelopes were slowly varied to achieve the piecewise adiabatic passage, as shown in Fig. 1(a).

Another conventional AP known in a three-level system is a chirped Raman passage (CRP) [6]. In CRP, the smooth pump and dump laser pulses share a similar temporal intensity profile, however, both pulses are frequency chirped, so that their carrier phases are $\phi_{P,D}(t) = \omega_{P,D}t + \alpha_{P,D}^{(\omega)}(t - t_0)^2/2$. Like STIRAP, CRP transfers population from state $|1\rangle$ into $|3\rangle$ in a robust manner; unlike STIRAP, CRP creates transient population in the state $|2\rangle$. For the piecewise version, all pulses are exactly on resonance. The effect of the frequency sweep is mimicked by varying the carrier phase of each pulse $\phi_{P,D}^{(0)}(n) = \phi_{P,D}(n, t) - \omega_{P,D}t$ quadratically with the pulse number n :

$$\phi_{P,D}^{(0)}(n) = \alpha_{P,D}(n - n_0)^2/2 \quad (1)$$

as shown by the staircase line in Fig. 1(b). Pulse trains with such a piecewise chirp have been used in Ref. [9] to demonstrate piecewise adiabatic following in a two-state system. Here we observe that the piecewise CRP in a three-level system is robust with respect to the field strengths, the number of pulse pairs, the values and signs of α_P and α_D , and to additional delays between the centers of the pump and dump pulse trains.

In both foregoing examples, the details of the single pulse dynamics are not important, only the values of the basis state amplitudes after each τ_n matter. Based on this observation, below we extend the conceptual scheme of PAP, generalizing the eigenstate $|2\rangle$ to a multitude of states, forming a wave packet. This wave packet undergoes complex dynamics between the pairs of pump and dump kicks, but if the pulse repetition time coincides with a revival, the wave packet (almost) returns to its original state by the time the next pair of pump and dump kicks arrives. The kicks, in turn, become rather

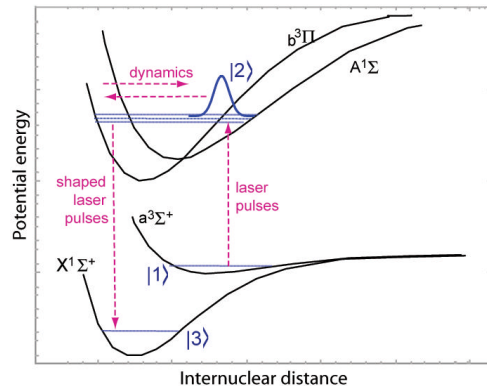


FIG. 2: (Color online). KRb potentials, basis states, and PAP arrangements discussed in the text.

complex operations implemented via an interplay of the shaped femtosecond pulses with the intermediate wave packet dynamics. We expect that, as long as the action of the kicks on the basis states $|1\rangle$, $|2\rangle$, and $|3\rangle$ mimics that of the dressing fields in the reference AP coarse-grained over τ_n , the enforced population transfer will be as robust with respect to the particular parameters of the kicks as that of the original AP with respect to the parameters of its dressing fields. Further, while matching the repetition time to the wave packet revivals enables a clear intuitive picture of the process, high fidelity of the revivals is not a necessary requirement, as we demonstrate later with unshaped pulses.

We test this idea via simulation of dynamics in KRb molecules, which is of special interest because of the prospect for creating ultracold polar molecules starting from loosely bound Feshbach states [10, 11]. As translationally and vibrationally cold polar molecules are a prerequisite in many applications [12], their robust high-yield creation is a forefront goal in cold matter research. However, for the sake of demonstrating the concepts described above, this example can be viewed as a generic molecular problem with rich dynamics that allows for convincing simulations.

The molecular potentials used in our simulations are shown schematically in Fig. 2. Eigenenergies and transition strengths are calculated using the algorithm FDEXTR [13] with the data input from Refs. [14, 15]. The excited electronic state is modeled as the LS-coupled $A^1\Sigma$ and $b^3\Pi$ potentials. Although the model is too simple to accurately describe molecular dynamics on the sub-microsecond time scale involved, it retains the main physical complexity of the problem due to the coupled singlet-triplet evolution. In our simulations we choose $|1\rangle$ to be the vibrational eigenstate $v = 5$ ($E = -7.14 \times 10^{-4}$ a.u.) of the $a^3\Sigma^+$ potential (Fig. 2). To trace the fidelity of the method, we also consider the amplitudes of vibrational eigenstates around the input state ($v = 0, 1, \dots, 12$ of the

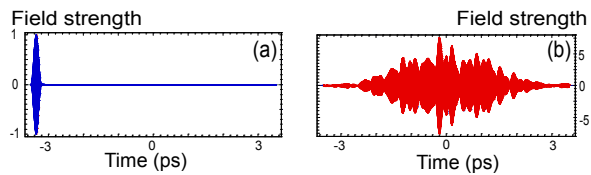


FIG. 3: (Color online) Time-dependent field of the pump (a), and dump (b) pulses. The field in each pulse is normalized relative to the maximum of the pump field.

$a^3\Sigma^+$ potential). The wave packet $|2\rangle$ is composed of up to 20 vibrational states of the LS coupled $A^1\Sigma-b^3\Pi$ potentials with the energies $E = 5.03 \times 10^{-2} - 5.2 \times 10^{-2}$ a.u. State $|3\rangle$ is the eigenstate $v = 22$ ($E = -1.134 \times 10^{-2}$ a.u.) of the ground $X^1\Sigma^+$ potential; the neighboring $X^1\Sigma^+$ eigenstates $v = 16, \dots, 28$ are included in the simulations as well.

The system, initially in state $|1\rangle$, is driven by a series of mutually coherent pump and dump femtosecond pulses. A single 110 fs FWHM (300 fs full duration) $\sin^2 \alpha t$ -shaped pump pulse, shown in Fig. 3(a), excites an $A^1\Sigma-b^3\Pi$ wave packet, which later undertakes irregular dynamics on the coupled $A^1\Sigma-b^3\Pi$ potential surfaces. At certain times it revives with a fidelity reaching ~ 0.9 . Following its excitation, the wave packet can be dumped into the single vibrational level $|3\rangle$. The shape of the femtosecond dump pulse is found by requiring that the wave packet before dumping overlaps well with the wave packet that would have been excited by the time-reversed dump, in a manner similar to the prescription of Ref. [3]. The thus-found dump field is shown in Fig. 3(b).

The simulation results for both piecewise STIRAP and piecewise CRP are presented in Fig. 4. For the piecewise STIRAP process, shown in Fig. 4(a,b), the field consists of 200 pairs of pump and dump pulses, each pulse shaped as in Fig. 3. The trains envelopes depend linearly on the pulse number, as shown in Fig. 4(a). The inter-pair separation is equal to 1310.59 ps (close to the time of revival of the wave packet $|2\rangle$). The carrier frequencies are chosen to match the Raman condition $\omega_{Raman} = \omega_P - \omega_D$. As prescribed in [2], the carrier optical phase is kept constant throughout each pulse train by choosing the carrier frequency to coincide with a comb tooth:

$$\omega^{P,D} = 2\pi(N^{P,D}f_{rep} + f_0^{P,D}) \quad (2)$$

where f_{rep} is the common repetition frequency and $f_0^{P,D}$ is the carrier-envelope offset frequency in the pump (dump) train.

If the spontaneous decay of the $A^1\Sigma-b^3\Pi$ states is neglected, the calculation predicts transferring 92% of population from $|1\rangle$ into $|3\rangle$. Introducing a 15-ns time scale for the decay of population from the $A^1\Sigma-b^3\Pi$ vibrational states reduces the transfer efficiency to 75%. The maximum combined transient population of all the $A^1\Sigma-b^3\Pi$

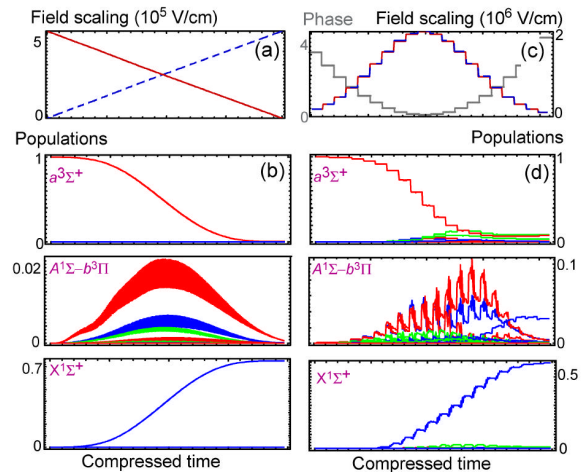


FIG. 4: (Color online) Dynamics of the STIRAP-like (a,b) and CRP-like (c,d) PAP in KRb. (a,c): Envelopes of the pump (dashed blue) and dump (red) pulses. Each point shows the factor by which the field shown in Fig. 3 is scaled. The carrier phase $\phi^{(0)}$ in the piecewise CRP, same for the pump and dump, is shown by the gray staircase in (c). (b,d): Population dynamics of all the levels in the system. Time is given at the “compressed” set of points: output is shown only for the times when the field is on. In each panel populations of different eigenstates of the corresponding manifold are shown by different colors.

levels reaches ~ 0.04 . A key observation is that population transferred to all other $a^3\Sigma^+$ or $X^1\Sigma^+$ eigenstates, except $|1\rangle$ and $|3\rangle$ is negligible. The transfer is found to be robust with respect to the number of pulses in the trains and their field strength profiles.

Figure 4(c,d) shows an example of the CRP-like PAP. The field consists of 20 pairs of pump and dump pulses. The pump and dump pulse train envelopes are Gaussian, as shown in Fig. 4(c). The inter-pair separation is equal to 1309.93 ps. The central carrier phase in each field evolves with the pulse number according to Eq.(1), with $\alpha_P = \alpha_D = 0.09$. The calculation with decaying $A^1\Sigma-b^3\Pi$ levels predicts transferring 60% of the initial population into the target state. (Neglecting the $A^1\Sigma-b^3\Pi$ decay raises this number to 65%). Approximately 2% of the population ends up distributed among eigenstates other than $|3\rangle$ of the target $X^1\Sigma^+$ manifold; 22% of the initial population are transferred to neighboring states of $|1\rangle$ in the $a^3\Sigma^+$ manifold at the end of the process. Unlike in the simple 3-level case, CRP-like transfer in the molecule is found to be significantly more sensitive than the STIRAP-like transfer, to the scaling of the pump and dump intensities, the number of pulses in the trains, and the intensity profiles of the trains. It should be noted that the required train envelope modulations (either in amplitude or phase) can be readily generated experimentally by present fast modulators for standard 1-10 ns repetition-period pulse sources.

The dependence of the transfer efficiency on ΔT in both STIRAP-like and CRP-like PAP is irregular because of the complex dynamics of the $A^1\Sigma-b^3\Pi$ wave packet and imperfection of its revivals. This dependence may be easier understood if viewed from the spectral perspective. In that view, each of the $A^1\Sigma-b^3\Pi$ eigenstates can serve as an intermediate level for a separate AP pathway. Reminiscent of the traditional coherent control via a wave packet [5, 16], the AP pathways interfere to provide the population transfer into the target state $|3\rangle$. Thus the frequency comb source drives a coherently controlled AP process [1, 4] via the set of intermediate $A^1\Sigma-b^3\Pi$ levels. Matching the repetition time and carrier phase to the wave packet revival time and phase ensures that all the possible AP pathways participate; spectral shaping of the pump and dump pulses sets constructive interference among the pathways.

Tailoring the optimal pulses requires detailed knowledge of the excited state structure, which is not always available. But what happens if the pulses are not shaped at all? Since coherent accumulation is highly selective spectrally, it is possible that the desired components of the intermediate wave packet are enhanced, while others are suppressed via Ramsey interferences. Fig. 5 investigates the total efficiency of the STIRAP-like transfer under *both* pump and dump trains consisting of 50 $\sin^2 \alpha t$ -shaped pulses, with respect to the inter-pair delay $\Delta T = 1/f_{rep}$ and intra-pair delay δT between the pump and dump pulses. Raman resonance is maintained throughout the f_{rep} scan by varying the carrier-envelope frequency difference according to $f_0^P - f_0^D = (\omega_{Raman}/2\pi) - Nf_{rep}$. The two-dimensional plot shows a remarkable landscape of vertical and horizontal features, where some peaks reach 80% transfer efficiency.

To elucidate some of the observed structure, consider δT , the relative time shift between the two trains, which is expressed in frequency as a linear spectral phase of the dump comb with respect to the pump comb. Accordingly, the phase of a specific Raman path at detuning Ω_i from the carrier frequency is $\varphi(\Omega_i) = -\Omega_i\delta T + \phi_d(\Omega_i)$, where $\phi_d(\Omega_i)$ is the relative phase of the dipoles associated with this path. The vertical lines in the image correspond therefore to a ΔT value where one or several teeth are in one-photon resonance with Raman paths. Changing δT at this ΔT reveals interference between these paths. A Fourier transform with respect to δT reveals the spacing between the intermediate levels, as shown in Fig. 5(b,c), where mostly two Raman paths, via $E_2^{(1)} = 5.08$ a.u. and $E_2^{(2)} = 5.1$ a.u., contribute and the Fourier transform of the transfer efficiency peaks at the beat frequency between $E_2^{(1)}$ and $E_2^{(2)}$. Horizontal lines, on the other hand, occur when δT hits a special value, where $\varphi_d(\Omega_i) \approx \Omega_i\delta T$ for the participating Raman transitions; i.e., δT is matched to the vibrational dynamics. In this case the transfer peaks even if there

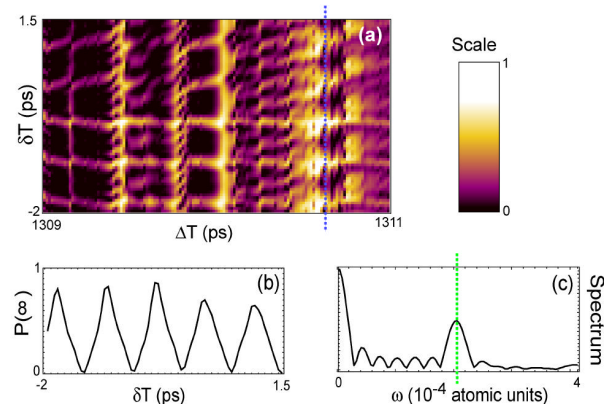


FIG. 5: (Color online)(a): An efficiency density plot for the STIRAP-like PAP with unshaped laser pulses in dependence on the inter-pair delay ΔT and the intra-pair delay δT . Positive δT indicates that the pump comes after the dump; i.e. population remains in the excited wave packet until the next dump comes (suffering more spontaneous emission losses). (b): Vertical at $\Delta T = 1310.62$ ps (blue dotted line in (a)). (c): Fourier transform of (b). The green dotted line marks the beat frequency between $E_2^{(1)}$ and $E_2^{(2)}$.

is no coherent accumulation in the intermediate levels, as was observed already in [3]. Since the match to the dynamics is only approximate, the lines are not perfectly horizontal. In the best case scenario every dump pulse transfers into $|3\rangle$ exactly all the population excited to $|2\rangle$ from $|1\rangle$ by the preceding pump [3].

With some preliminary knowledge of the initial and target state's eigenenergies, the range of frequencies and the field strengths needed (but not of the exact values of intermediate eigenenergies and transition dipoles involved), one can take trains of unshaped pump and dump pulses, and scan ΔT and δT to find efficient PAP transfers. In an analogy with 2D Fourier spectroscopy [17], a theoretical analysis of the 2D scan of the transfer efficiency may be able to provide the full spectroscopic information. Further, one can experimentally optimize the pulse shapes in order to maximize the transfer fidelity.

We are pleased to thank V. Milner, I. Thanopoulos, and S. Kotochigova for discussions and consultations. The work at JILA was supported by NIST and NSF.

-
- [1] M.C. Stowe *et. al.*, Adv. At. Mol. Opt. Phys. **55**, 1 (2007); M.C. Stowe *et. al.*, Phys. Rev. Lett **96**, 153001 (2006).
 - [2] E.A. Shapiro *et. al.*, Phys. Rev. Lett. **99**, 033002 (2007).
 - [3] A. Pe'er *et. al.*, Phys. Rev. Lett. **98**, 113004 (2007).
 - [4] P. Kral, I.Thanopoulos, M. Shapiro, Rev. Mod. Phys. **79**, 53 (2007).

- [5] M. Shapiro and P. Brumer, *Principles of the Quantum Control of Molecular Processes* (Wiley & Sons, NY, 2003).
- [6] J. Oreg, F.T. Hioe, J.H. Eberly, Phys. Rev. A **29**, 690 (1984).
- [7] U. Gaubatz *et. al.*, J. Chem. Phys. **92**, 5363 (1990); N.V. Vitanov *et. al.*, Adv. At. Mol. Opt. Phys. **46**, 55 (2001), and references therein.
- [8] Using the data from NIST Atomic Spectra Database, (<http://physics.nist.gov/PhysRefData/ASD/>), we took $\mu_{12} = 2.5$ a.u., and $\mu_{23} = 3$ a.u. The field-free decay and ionization by the field are negligible under the conditions shown in the Figure.
- [9] S. Zhdanovich *et. al.*, arXiv:0710.3145v1 [physics.atom-ph] (2007).
- [10] T. Köhler, K. Góral, P.S. Julienne Rev. Mod. Phys. **78**, 1311 (2006), and references therein.
- [11] J. J. Zirbel *et.al.*, arXiv:0710.2479 [cond-mat].
- [12] J. Doyle *et. al.*, European Physical Journal D **31**, 149 (2004), and references therein; A. Micheli, G.K. Brennen, P. Zoller, Nature Physics **2**, 341 (2006).
- [13] A.G. Abraskevich, D.G. Abraskevich, Computer Physics Communications **82**, 193 (1994); *ibid.*, **82**, 209 (1994).
- [14] S. Rousseau, A.R. Allouche, M. Aubert-Frecon, J. Mol. Spectrosc. **203**, 235 (2000); <http://lasim.univ-lyon1.fr/allouche/pec.html>
- [15] S. Kotochigova, E. Tiesinga, P.S. Julienne, Eur. Phys. J. D **31** 189 (2004); S. Kotochigova, P.S. Julienne, E. Tiesinga, Phys. Rev. A **68** 022501 (2003).
- [16] A. Stolow, Phil. Trans. Roy. Soc. A **356** 345 (1998).
- [17] D. M. Jonas, Annu. Rev. Phys. Chem. **54**, 425 (2003).